Chapter 3

Metallic Glass Matrix Composite Honeycombs

Introduction

Recent discoveries in metallic glass matrix composites have resulted in some of the toughest materials known [23, 48]. These materials are the result of the realization that certain glass-forming systems can be solidified with an interspersed soft dendrite phase resulting in enhanced mechanical properties [49], and that the dendrite is chemically stable in the presence of the liquid so that semi-solid processing is possible and results in a controlled microstructure [50]. This control of the microstructure allows for a composite to be made where the spacing between the dendrites is smaller then the plastic zone size of the metallic glass matrix which allows shear bands to form in the glass and be interrupted by the soft dendrites before fracture occurs causing more shear bands to form in the glass, and so on, resulting in global ductility and the high strengths expected from metallic glass. The resulting materials have extraordinary properties with strengths up to $\sim$1.5 GPa and tensile ductility up to $\sim$10% strain to failure [23]. Further studies of in situ composites have shown that specimens fabricated by semi-solid processing

followed by techniques such as hot forging [51], cold rolling, and thermoplastic forming [52] maintain the extraordinary mechanical properties that are characteristic of these materials. These in situ composites are excellent candidates for use in cellular metals because of extraordinary mechanical properties, and the variety of available processing methods make it possible to fabricate interesting net shapes of the material.

As discussed in chapter 1, cellular metals have been studied extensively because of the interesting collection of properties including relatively high strength and stiffness at low densities and high energy absorption [24]. The properties of periodic cellular structures made from a bulk metallic glass were investigated in chapter 2, and were shown to exhibit strengths much higher and energy absorption capabilities nearly 100 times better than stainless steel honeycombs. Because these new metallic glass matrix composites have comparable strengths and ductility well beyond that seen in metallic glass, they should be excellent materials for use in cellular structures.

The design of a cellular structure made from these metallic glass matrix composites is similar to that for bulk metallic glass structures, but yielding by brittle fracture should not be a problem because the plastic zone size of the composites is on the order of millimeters [23]. Elastic buckling, however, could still be an issue, so the slenderness ratio of struts must be restricted. Following analysis carried out in chapter 2, the critical slenderness ratio, $(L/r)_{cr}$, is found to be between about 10 and 50 which is the same range as for BMG struts because the yield strain, $\varepsilon_y = E/\sigma_y$ is about 0.02 for both materials.

Methods

Corrugated sheets and egg-box structures of a metallic glass matrix composite alloy with composition $Zr_{36.6}Ti_{31.4}Nb_7Cu_{5.9}Be_{19.1}$ were fabricated by semi-solid induction forging under an argon atmosphere with water cooled copper dies as described in reference [51]. The dies for these sheets were designed to make an equilateral triangle honeycomb-type structure similar to the bulk metallic glass (BMG) cores of the previous chapter. Corrugated sheets with struts of thickness between 0.47 and 0.85 mm and resulting slenderness ratios of 10 or less and egg-box structures with relative densities as low as 11% were used in this study. The sheets were characterized using XRD to ensure that the amorphous and bcc phases were present in the as formed material, as shown in figure 3.1 (from [51]). The sheets were cut into rectangular strips, the compressed faces were ground plane parallel prior to testing. Single cores and two-core stacks were compressed quasi-statically in the in-plane configuration and single cores were compressed in the out-of-plane configurations with an applied strain rate of 10^{-3} s^{-1}. Compression experiments for the egg-box structures were also carried out at an applied strain rate of 10^{-3} s^{-1}. Tests were carried out with a screw-driven Instron universal testing machine with a load capacity of 50 kN and displacements were measured with a linear variable differential transformer. The cores tested here range from 0.25 to 0.35 in relative density and the egg-boxes have relative densities around 0.12. The relative densities of the specimens were calculated using the density of the solid as-forged material (as measured by Archimedes' method) and the measured volume of the rectangular prism occupied by the specimen.

These corrugated strips and egg-boxes were compressed with flat tool steel plates as the top and bottom sandwich layers. The metallic-glass-matrix-composite (MGMC) structures were not bonded to the tool steel plates. For the two-core stacks, several materials were tested as the middle plate (tool

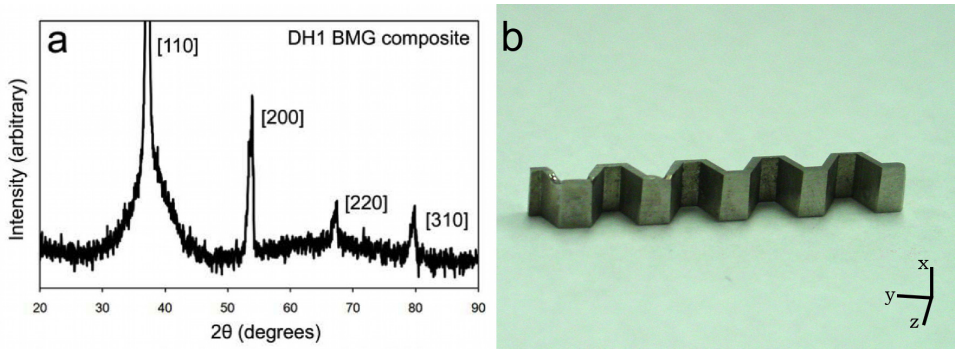

Figure 3.1: (a) XRD of as forged corrugation verifying phase character of the metallic glass matrix composite showing amorphous background and indexed bcc crystal peaks (from Hofmann et al. [23]). (b) Image of metallic glass matrix composite as prepared for quasi-static compression. The z-axis is the in-plane loading axis, and the x-axis is the out-of-plane loading axis.

steel, metallic glass matrix composite, and bulk metallic glass). The choice of mid plate did not, however, significantly alter the stress-strain behavior of the stacks. The data for two-core stacks presented here were gathered on specimens with a BMG or MGMC mid plate.

Results and Discussion

In-Plane Loading

The stress-strain response of quasi-statically loaded single cores and two-core stacks for in-plane and out-of plane loading is shown in figure 3.2. Images of a representative single core specimen during a compression test are shown in Fig 3.3(a) through (c). The single cores exhibit strains of 20% or greater before exhibiting a non-catastrophic collapse event, then load again and maintain a plateau of about half of the yield strength through to densification. Figure 3.3(b) shows that the primary failure event in an MGMC core is quite

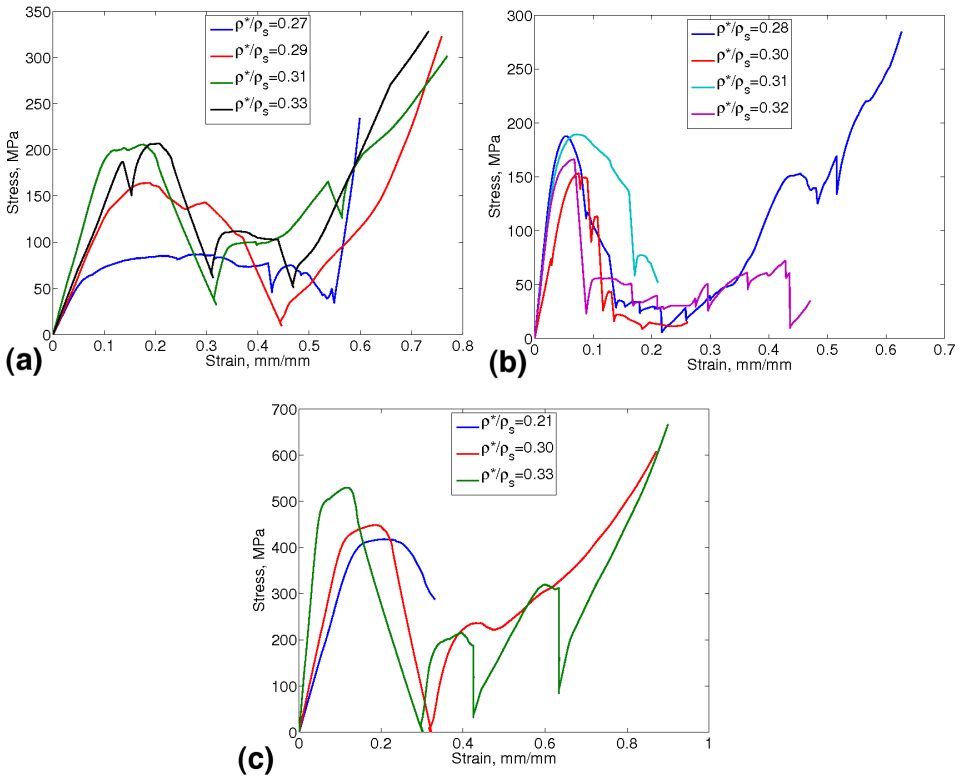

Figure 3.2: Stress-strain response of (a) single cores and (b) two-core stacks of MGMC corrugated sheets for quasi-static in-plane loading and (c) single cores in quasi-static out-of-plane loading.

localized and visually far less catastrophic than the similar image of metallic glass core in figure 2.7(c). Micrographs of compressed specimens seen in figure 3.3(d) and (e) also show macroscopic evidence of plastic deformation and a dense network of shear bands in the region of this deformation.

The two-core MGMC stacks show high yield stresses, but plateau stresses of only ∼25% of the yield stresses (figure 3.2(b)). Photographs of a stack of MGMC cores during a compression test are shown in figure 3.4. The collapse of one strut results a significant rearrangement of the nearby nodes. In the example shown in figure 3.4(b) this has resulted in the misalignment

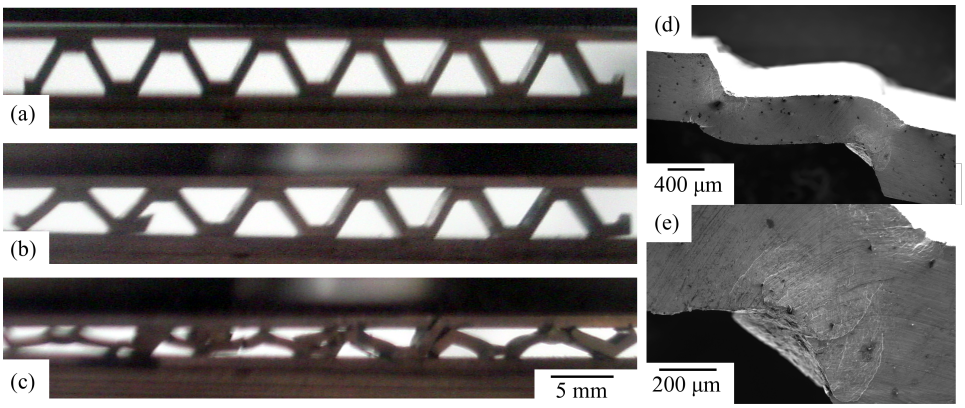

Figure 3.3: Images of a single core of the MGMC (a) in the elastic region, (b) after the first collapse event, and (c) near densification, and electron micrographs of a specimen after compression showing (d) severe plastic deformation and (e) a dense network of shear bands in the area of severe plastic deformation.

of several of the nodes. As the compression continues, the deformation is not uniform across the structure as nodes slide and rotate while the load is held by a small number of critical struts. Eventually the plateau stress rises, but only shortly before densification as seen in the stress-strain curve for the $\rho^*/\rho_s = 0.28$ specimen in figure 3.2(b).

The out-of-plane specimens show very high yield strengths and plateau stresses with stress dropping to very low values when collapse events occur (figure 3.2(c)). In the large plastic region just after yielding, these specimens show some buckling of cell walls prior to any collapse event. This buckling can be seen in figure 3.5(b). The initial collapse events in these in these samples result in a single huge shear band which cuts through the entire core as seen in figure 3.5(c). Further deformation in compression yields more large deformations along shear bands in the specimen, as seen in figure 3.5(d), in addition to more stable plastic deformation due to smaller shear bands

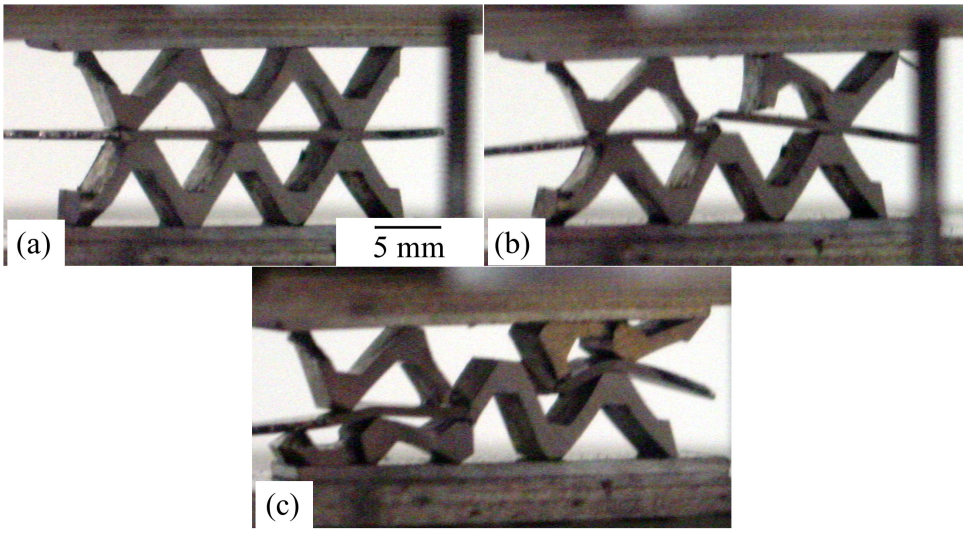

Figure 3.4: Images of a two-core stack of the MGMC (a) in the elastic region, (b) after the first collapse event showing that the nodes of the two cores are now misaligned, and (c) further deformation of the structure showing that the plastic deformation is not uniform across the structure.

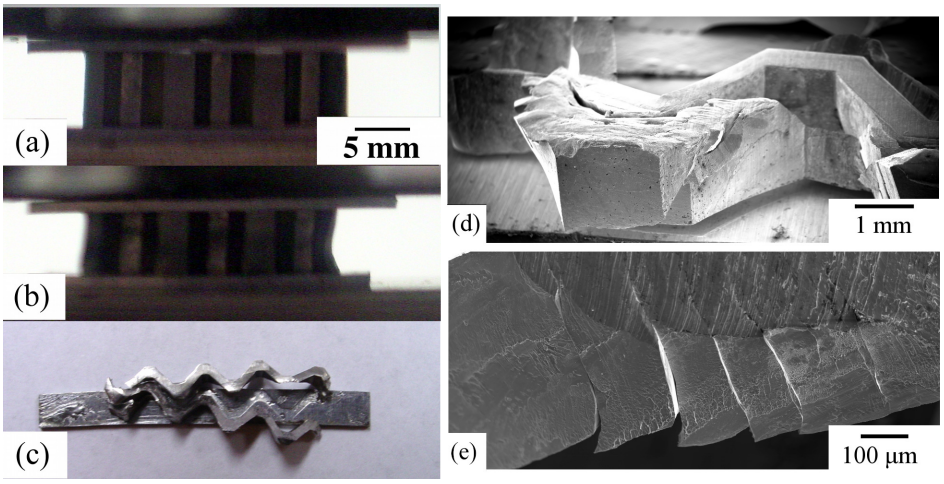

Figure 3.5: Images of out-of-plane MGMC specimens during testing (a) in the elastic region and (b) showing plastic buckling in the plateau after yielding and (c) top view after the first collapse event. Electron micrographs of an out-of-plane MGMC specimen: (d) side view showing massive deformation along large shear bands and (e) shear bands on top compression surface.

seen in figure 3.5(e) between collapse events. The collapse events in these specimens appear to have the same nature as the collapse events seen in the metallic glass cores in chapter 2 in the sense that when the dominant shear band travels through the specimen, it affects multiple struts and treats the corrugated sheet as a monolithic specimen, and not a collection of connected columns. The fact that the shear band affects the entire MGMC core and affects only several struts in the BMG cores is probably because the slenderness ratio of the typical strut, and therefore the relative density, of the MGMC cores is several times that of the BMG specimens, so the core loaded out-of-plane is effectively more like a thick column of uniform cross section.

The egg-box is a more porous structure, which using the same processing technique results in a lower density structure. The cell walls in the egg-box are also constrained along three edges as opposed to the corrugated sheets

where the cell walls have only two parallel constrained edges, so the structure is a bit more stable against buckling. As seen in figure 3.6(a) and (b), these structures are able to deform to full densification while remaining largely in one piece. The stress-strain response (figure 3.6(c)) shows a peak in stress much like the other MGMC structures, but the drop in load is not nearly as precipitous, and the plateau is relatively uniform in stress. The less severe drop in stress after the peak is attributed to the geometry of the structure as the cells fully span only the vertical dimension of the structure so when one cell wall fails, a smaller portion of the specimen is affected. In the case of the single core specimens, each cell spans both the height and the depth of the specimen, so when one strut breaks, it affects a large part of the structure. The stress drop could be further ameliorated by using specimens with even larger numbers of cells.

The relative strength-relative density relationships for MGMC corrugations are shown in figure 3.7. In-plane structures show an exponent of $n = 0.84$ that does not seem to correspond with any of the relative strength-relative density relations presented in ref. [24]. The data span only a small range of relative densities and show a bit of scatter, so the power law fit is not very good and the mechanism of failure cannot be determined by this method. As these materials are known to show ductility in tension [23], and the images in figures 3.3 and 3.4 show macroscopic and microscopic evidence of plastic deformation, the expected mechanism of yielding for an in-plane MGMC structure is plastic yielding of its struts.

The out-of-plane cores show strengths several times higher than in-plane structures with a fit exponent of $n = 1.58$ which, as discussed in chapter 2 corresponds to plastic buckling of cell walls in out-of-plane loading. These data also span only a small range of relative densities, but they show a clear trend and the power law fits them well. This buckling can be seen in

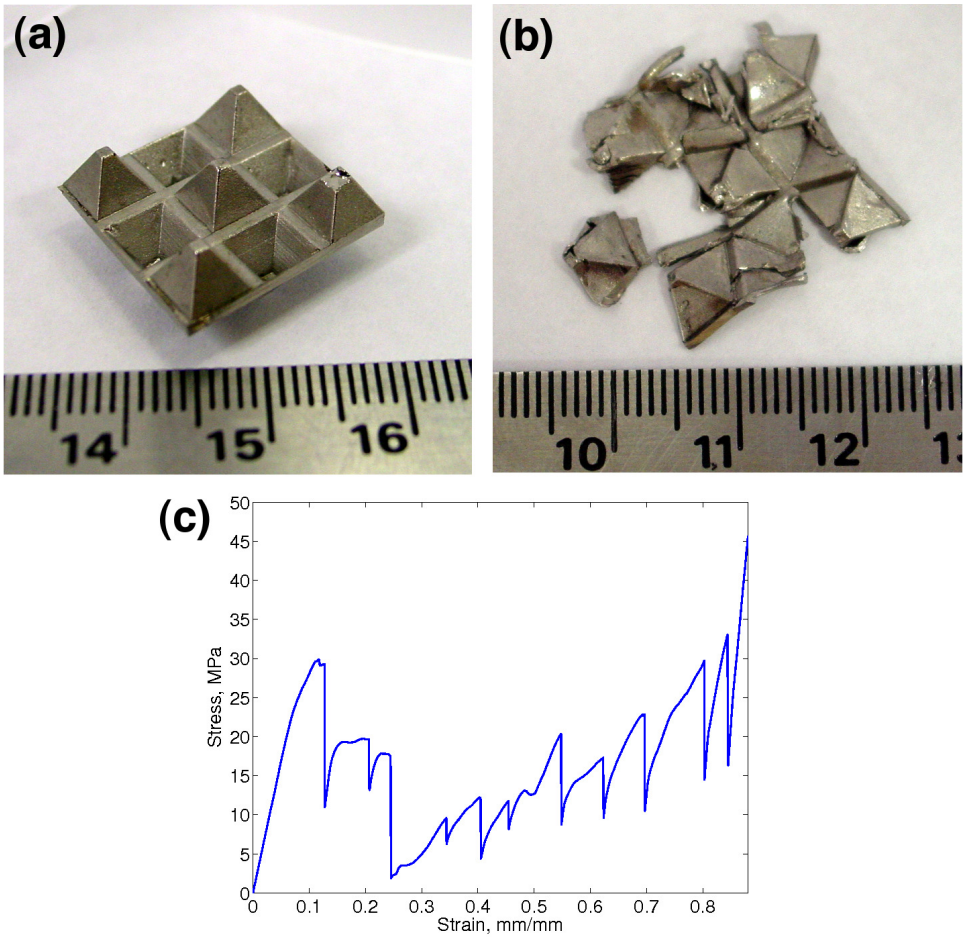

Figure 3.6: Images of an MGMC egg-box structure (a) as prepared for testing and (b) after testing showing the ability to flatten almost completely and remain largely in one piece. (c) Stress-strain response of a representative egg-box with $\rho^*/\rho_s = 0.12$.

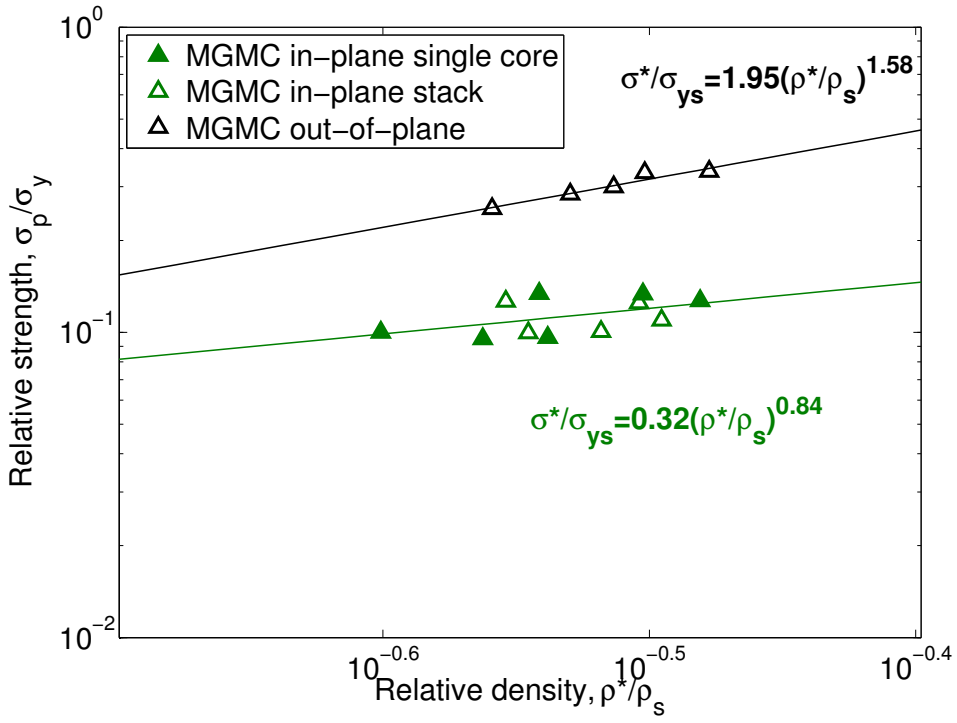

Figure 3.7: Relative strength-relative density plot for MGMC structures in in-plane and out-of-plane loading. Lines are power law best fits to the data.

figure 3.5(b), and micrographic evidence of the plastic nature of the yielding in the form of shear bands can be seen in figure 3.5(d) and (e), so the out-of-plane MGMC cores definitely yield plastically.

When these structures are compared to the data for existing structures made from stainless steel, as in figure 3.8, the MGMC shows strengths 4–5 times higher than for steel structures of nearly the same relative density with very high sustained plateau stress. The curve for the out-of-plane MGMC in figure 3.8(b) shows a total strain of about 35% as opposed to almost 80% for the steel because this test was carried out only until the first collapse event and not to densification. The stress-strain response of the 12% dense egg-box structure is higher in stress in almost every respect to an 8% dense stainless steel honeycomb and shows significantly higher peak stress and roughly equal sustained plateau stress when compared to a stainless steel honeycomb with 19% relative density, as seen in figure 3.8(c).

Comparing MGMC structures with those made from crystalline metals and the BMG structures over a range of relative densities, we can see that the peak strength of MGMC structures falls generally in line with the peak strength of the BMG structure for both in-plane and out-of-plane loading, which is significantly higher than the strength exhibited by stainless steel structures in in-plane and stainless steel and aluminum structures in out-of-plane loading over a range of relative densities (figure 3.9). The egg-box structures are plotted with the in-plane structures as their cell walls are also loaded in a bending mode and not in compression like for out-of-plane loaded honeycombs. The higher strength of the metallic glass and composite structures is the result of the higher strength of metallic glass and composite parent materials.

Energy absorption of the MGMC structures was calculated in the same manner as the for BMG structures in chapter 2. The energy absorption

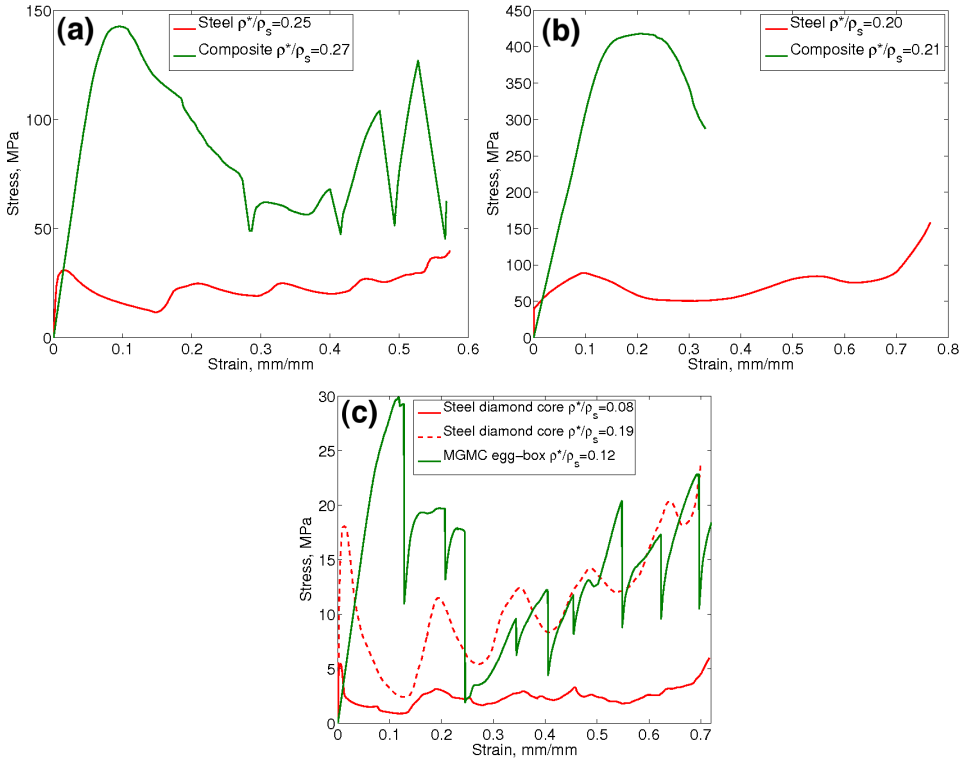

Figure 3.8: Stress-strain plots comparing the behavior of MGMC structures with steel structures of roughly the same density and similar geometry for (a) in-plane honeycomb, (b) out-of-plane honeycomb, and (c) egg-box structures. Steel data from refs. [46, 47]

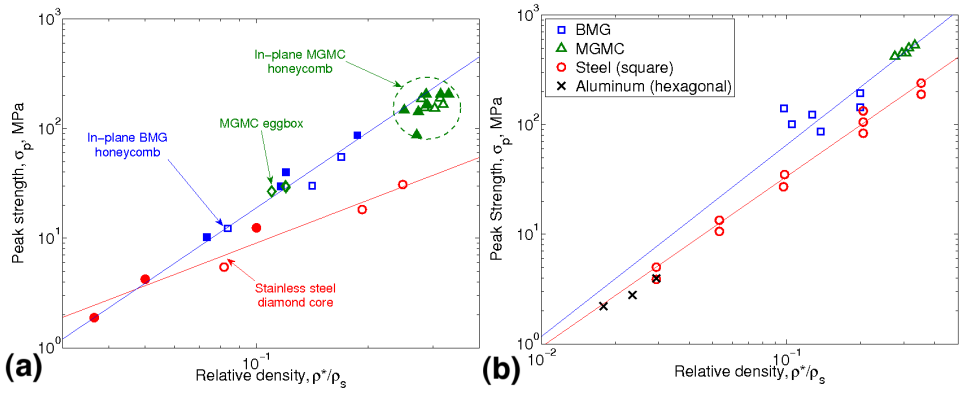

Figure 3.9: Strength-relative density plots for BMG and MGMC structures and crystalline metal structures under (a) in-plane and (b) out-of-plane loading. Steel and aluminum data from refs. [46, 47]

capabilities of the MGMC structures are shown in figure 3.10. The composite structures are capable of absorbing between three and five times more energy than structures made of crystalline metals for both honeycomb loading configurations. Again, the egg-box structures are plotted along side the in-plane honeycombs, and they show at least a fivefold increase in energy absorption over steel honeycombs of the same relative density. This high energy absorption is the consequence of the high strength of the metallic glass matrix composite material, and the ability of the structure to collapse non-catastrophically allowing it to maintain a high plateau stress throughout densification.

The plateau stress is quite an important property in the selection of an energy absorbing structure, as it determines the stress that is transmitted through the structure to whatever it is that the structure is trying to protect. figure 3.11 shows the energy absorbed per gram of structure in relation to the plateau stress. For a selected plateau stress, the MGMC structures absorb 4 to 5 times as much energy per gram of structure than the stain-

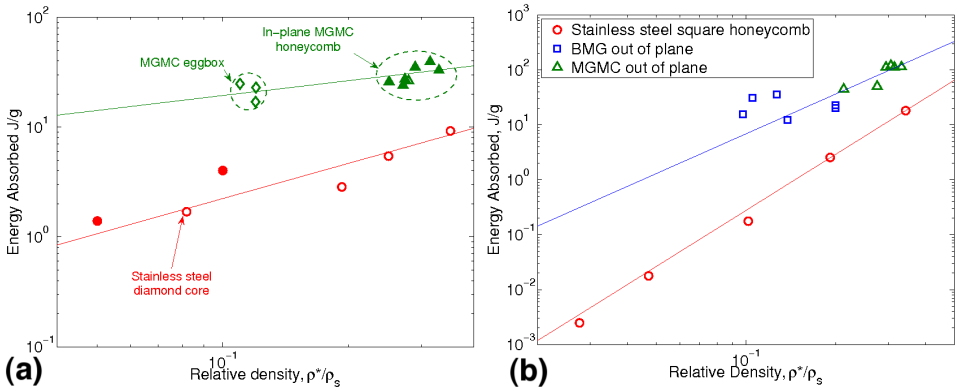

Figure 3.10: Energy absorbed per unit mass versus relative density plots for BMG and MGMC structures and crystalline metal structures under (a) in-plane and (b) out-of-plane loading. Steel data from refs. [46, 47]

less steel honeycombs. From the perspective of this materials selection plot, the MGMC structures beat the steel structures because the MGMC parent material has much higher yield strength than stainless steel and it is also significantly lighter (5.68 g/cm^3 for $Zr_{36.6}Ti_{31.4}Nb_7Cu_{5.9}Be_{19.1}$ compared to 8.00 g/cm^3 for the 304 stainless steel used in the structures from Côté et al. [46, 47]).

Conclusion

Periodic structures have been produced from in situ metallic glass matrix composites using a semi-solid induction forging technique, and their mechanical properties examined for both in-plane and out-of-plane configurations. Egg-box structures have also been produced from the MGMC and tested. These structures have relative densities ranging from $\rho^*/\rho_s = 0.11$ to $\rho^*/\rho_s = 0.35$. Because of the narrow range of relative densities for the honeycombs (ρ^*/ρ_s =0.25 to 0.35, it is difficult to glean the yielding mechanism

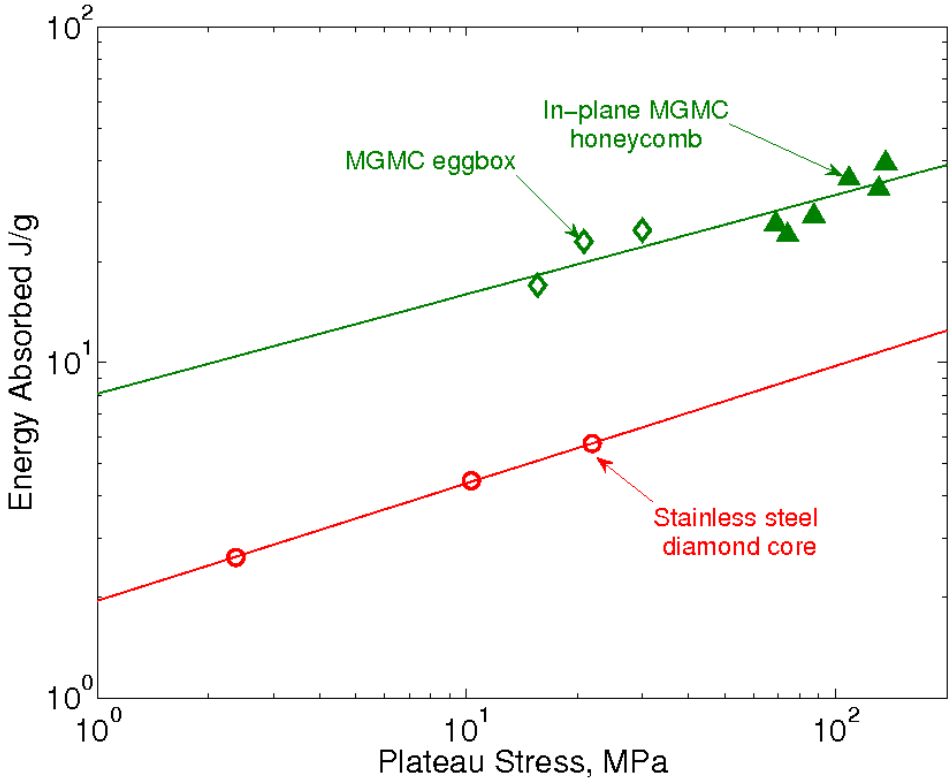

Figure 3.11: Energy absorbed per unit mass versus plateau stress for MGMC structures and crystalline metal structures showing very high energy absorption capabilities of MGMC structures. Steel data from ref. [46].

from the relative strength–relative density relationship, but the material is ductile, micrographs show evidence of plastic deformation, and the struts are far too thick to buckle elastically, so the yielding mechanism of these structures is believed to be plastic yielding. The metallic glass matrix composite structures show strengths that are several times stronger than steel structures of the same relative density in both in-plane and out-of-plane loading. The energy absorption capabilities of these materials are just as impressive as those for metallic glass structures absorbing from several times to almost 10 times more energy than steel structures of the same relative density with stress plateaus that are more uniform than those of the metallic glass structures, but it is believed that they could be even better with further optimization of the structural geometry. Egg-box structures show slightly larger gains in strength and energy absorption over steel structures than do the honeycombs. These structures are lightweight and very strong with very high capacity for energy absorption.